An Integrated Multimodality MR Brain Imaging Study: Gray Matter Tissue Loss Mediates The Association Between Cerebral Hypoperfusion and Alzheimer's Disease

Duygu Tosun, Norbert Schuff, and Michael Weiner

Abstract— **Multimodality MR image processing and analysis aims to determine to what extent information from various imaging modalities is redundant or complementary and how changes in various regions of the brain, detected by various modalities, interact with each other to produce cognitive and functional changes. Here, we presented a multimodality image processing framework to integrate unique and complementary observations on anatomical and physiological brain changes measured by structural and perfusion MR imaging modalities. A unique aspect to this study is that we performed a test on mediation hypothesis that requires a model based on measurements from both MR imaging modalities. Our findings from these integrated multi-modality analysis were congruent with previously published results on neuropathology of AD patients and supplied a comprehensive explanation on the integration between structural atrophy and physiological deterioration due to AD.**

I. INTRODUCTION

Neurodegenerative brain diseases possess unique morphological signatures; detection of such signs may prove useful in improving diagnosis, particularly for diseases in which there are few other diagnostic tools. Developments in medical imaging techniques, particularly in the main anatomical imaging modalities magnetic resonance imaging (MRI), computed tomography (CT), and diffusion weighted MRI (DWI) and the main physiological imaging modalities positron emission tomography (PET), functional MRI (fMRI), perfusion MRI have allowed for in vivo imaging studies concerning the structure and function of the human brain on large number of subjects. Until now, most studies have been pursuing the traditional uni-modality group analysis approach, where data from a single imaging modality from groups of subjects are compared in a standard space (e.g., voxel-based morphometry, deformation-based morphometry) [1]. With the recent advances in acquisition methods and image processing methodologies, a major challenge is to develop better analysis methods to use multiple imaging modalities together for improved diagnosis and greater information concerning the changes in the brain that are responsible for cognitive and functional changes.

Here, we present a study on multimodality MR brain imaging data set to gain more information concerning the changes in the brain, which occur in neurodegenerative diseases. We are specifically interested in neurodegenerative diseases associated with dementia in the elderly, such as Alzheimers disease (AD). Neuropathology of AD includes structural gray matter (GM) atrophy in temporal, parietal, and frontal cortices [2], [3], [4], functional changes prominently in the parietal cortex (including the posterior cingulate gyrus and lateral parieto-temporal areas) [5], [6], and altered white matter (WM) fiber integrity in parietal, temporal, and frontal cortices [7], [8], [9]. Until now, the association between AD and imaging variables have only been investigated with pair-wised approaches (i.e., AD diagnosis versus tissue atrophy, deteriorated brain function or WM fiber integrity). A co-analysis approach to identify brain regions where structural and functional changes occur in concordance or in dissociation was proposed in [10], though the proposed analysis was based on statistical significances again from pair-wised comparisons. Limited work has been done to provide comprehensive explanation to the interaction between structural and functional pathologies in AD.

In this work, we aimed to test the hypothesis that the cerebral hypoperfusion, by affecting the oxygen and glucose delivery, may create optimal conditions for the progression of the neurodegenerative process (i.e., atrophy) of AD [11], [12], [13]. In particular, we engineered an integrated multimodality MR image processing and analysis framework to determine whether cortical GM atrophy mediates the association between AD diagnosis and cerebral hypoperfusion. We investigated local changes in GM thickness and cerebral perfusion, obtained by T1-weighted structural MRI and continuous arterial spin labeling (cASL) perfusion MRI, respectively. The main image processing challenges we addressed in this framework are the spatial alignment of the intra-subject inter-modality MR images and the partial volume effect correction on the perfusion data with respect to the underlying structural imaging data, which allows us to perform the mediation test at points densely distributed on the cerebral cortex tissue (i.e., 3D cortical surface-based data analysis). To our knowledge, this is the first investigation on structural and functional neuropathologies in AD using an integrated multimodality image processing framework coupled with 3D cortical surface-based data analysis.

II. METHODS

Data Acquisition.   All scans were performed on a 4 Tesla (Bruker /Siemens) MRI system with a birdcage transmit and 8 channel receive coil.

D. Tosun is with the Center for Imaging Neurodegenerative Diseases, VA Medical Center (114M), 4150 Clement St., San Francisco, CA 94121 USA. `duygu.tosun@ucsf.edu`

M. Weiner is with the Center for Imaging Neurodegenerative Diseases, VA Medical Center (114M), 4150 Clement St., San Francisco, CA 94121 USA.

T1-weighted images were obtained with a 3D volumetric magnetization prepared rapid gradient echo (MPRAGE) sequence, TR/TE/TI = 2300/3/950ms, timing; 7° flip angle; $1.0 \times 1.0 \times 1.0$ mm^3 resolution; 157 continuous sagittal slices; acquisition time of 5 min. T2-weighted images were acquired with variable flip (VFL) angle turbo spin-echo sequence with TR/TE = 4000/30ms and with the same resolution matrix and field of view of MPRAGE.

Perfusion MR brain images were acquired based on a continuous arterial spin labeling (cASL-MRI) sequence [14]. cASL-MRI data were acquired using single-shot echo-planar imaging (EPI), consisted of five 5-mm-thick slices with 24% gaps, with an in-plane resolution of 3.75×3.75 mm^2, oriented 10° up from the anteriorposterior commissural line and covered the volume above this line. The other acquisition parameters were as follows: TR/TE = 5,200/9 ms and 1,590 ms post labeling delay.

Structural MR Image Processing. The skull, scalp, extracranial tissue, cerebellum, and brain stem (at the level of the diencephalon) were removed from each image data using an automated method [15] followed by quality check. The remaining image volume was then corrected for intensity inhomogeneity using the non-parametric non-uniform intensity normalization (N3) technique [16]. These processing steps were followed by the reslicing of the remaining image volumes into a standard orientation of the International Consortium for Brain Mapping-305 (ICBM-305) average brain by a least-squares rigid body transformation. The global differences in brain size and shape remained intact during the transformation into the ICBM-305 average brain space. The resliced image volumes had isotropic voxels each having size of 1 mm×1 mm×1 mm. Each individual's cortical surface was extracted using a cortical reconstruction method using implicit surface evolution (CRUISE) technique developed by Han et al. [17] and shown to yield an accurate and topologically correct representation that lies at the geometric center of the cortical GM tissue [18]. CRUISE is a data-driven method combining a robust fuzzy segmentation method, an efficient topology correction algorithm, and a geometric deformable surface model. Each resulting cortical surface was represented as a triangle mesh comprising of approximately 300,000 mesh nodes.

Cortical thickness at each point in the cortical GM tissue mantle was defined as the sum of the distances from this point to the GM/WM and GM/cerebro spinal fluid (CSF) tissue boundaries following a flow field which guarantees a one-to-one, symmetric, and continuous correspondence between the two tissue boundaries. A flow field with these properties was computed by solving a Laplace's equation with cortical GM tissue mantle as its domain [19], [20]. Cortical thickness was estimated in millimeters at 3-D image voxels on the GM tissue mantle. Estimated cortical thickness values were mapped onto the corresponding central cortical surface using trilinear interpolation at each mesh vertex.

Cortical spatial normalization was used to match anatomically homologous cortical features across subjects. In particular, the central cortical surface model of each subject was spatially normalized with respect to the geometry of a representative reference brain (i.e., the colin27 average brain [21]) using an automated surface-based cortical warping method [22]. As a result, individual cortical morphometry measures from homologous surface locations were mapped onto the reference surface, where statistical analyses were carried out.

Perfusion MR Image Processing. For each subject, 39 repeat labeled images and 39 repeat references images were first rigidly re-aligned to the first labeled image and reference image, respectively. Re-aligned images were then averaged to generate a mean labeled image volume, $\mathrm{PWI_{labeled}}$, and a mean reference image volume, $\mathrm{PWI_{ref}}$. The mean labeled and reference images were then subtracted to obtain the perfusion-weighted image data, $\mathrm{PWI_{raw}}$.

The perfusion signal is proportional to the arterial water signal, requiring $\mathrm{PWI_{raw}}$ to be normalized by the arterial water density. However, it is virtually impossible to reliably sample the arterial water signal for every voxel. We substituted the signal from tissue density for the arterial signal. The reference image of cASL-MRI is a good representation of tissue water density for all practical purposes. The intensity normalized perfusion image was obtained by $\mathrm{PWI_{norm}} = \frac{\mathrm{PWI_{raw}}}{\mathrm{PWI_{ref}}}$. Normalization also addresses the intensity inhomogeneity and high frequency artifacts from residual vascular signal.

The final processing in the native perfusion imaging space was the scaling based on the model of perfusion to estimate the cerebral blood flow (CBF), which is given as

$$\mathrm{CBF} = \mathrm{PWI_{norm}} \times \frac{\lambda e^{\mathrm{R_{1app}} \mathrm{T_d}}}{2 \times \mathrm{R_{1app}}}, \tag{1}$$

where λ is the brain-blood partition coefficient for water (i.e., 0.95 mL/g), R_{1app} is the apparent relaxation rate, and $\mathrm{T_d}$ is the post labeling delay time. CBF is in units of mL/g per minute.

In neurodegeneration studies, we are interested in the blood flow in cerebral GM, which is bounded by CSF and WM tissue. CSF does not contribute to the perfusion signal, however, variable amounts of CSF within an image voxel, especially on the GM/CSF tissue interface, induce modulations on the perfusion signal. Moreover, perfusion on GM and WM tissue differ in magnitude, inducing additional modulations of the perfusion signal on the GM/WM tissue interface voxels. CBF image was corrected for GM/CSF and GM/WM partial volume effects. Intra-subject inter-modality spatial alignment was performed to bring CBF image to image space where tissue densities were defined (i.e., structural MR image space). One of the key challenges in inter-modality spatial alignment is the EPI-based perfusion image's susceptibility to nonlinear geometric distortion. We used a fluid-flow based distortion correction. In particular, both $\mathrm{PWI_{ref}}$ and CBF were first mapped onto T2-weighted structural image space using a multi-resolution affine registration algorithm based on normalized mutual information. Co-registered $\mathrm{PWI_{ref}}$ image was then fluid-flow warped to T2 image [23]. Resulting fluid-flow warping field

was applied to co-registered CBF image. Finally, T2 image was rigidly aligned to T1 image space, where the cortical geometry and thickness measure were defined. T2 to T1 rigid alignment transformation was then applied to the geometric distortion corrected CBF image, yielding CBF_{corr}.

Assuming that at each voxel the CBF_{corr} is a weighted combination of perfusion from GM and WM (i.e., CBF_{GM} and CBF_{WM}, respectively), and the weighting coefficients are directly proportional to the corresponding tissue density (i.e, β_i for $i = $ GM, WM), and the relationship between GM and WM perfusion is spatially constant (i.e, $CBF_{GM} = \kappa \times CBF_{WM}$), then the partial volume correction on the $rmCBF_{corr}$ is given by

$$CBF_{PVE} = \frac{\beta_{GM}}{\beta_{GM} + \beta_{WM}/\kappa} CBF_{corr}. \qquad (2)$$

Finally, for integrated multimodality data analysis, we generated cortical surface mapping of CBF_{PVE} by integrating the CBF_{PVE} values over a curvilinear line bounded by the GM tissue thickness at every surface mesh node.

Integrated Multimodality MR Image Analysis. A surface-based intrinsic isotropic diffusion was used to increase the signal-to-noise ratio before performing surface-based statistical analysis. In particular, the estimated value (cortical thickness or CBF_{PVE}) at each mesh node was replaced by the convolution of the measure map of interest with a Gaussian kernel centered at this mesh node. The Gaussian kernel domain was defined on each cortical surface over a geodesic neighborhood of radius 10 mm. The size of the smoothing kernel matched the size of the effect we sought while accounting for residual errors in the surface warping. For each subject brain, smoothed measure values at each surface mesh node were transferred onto the anatomically homologous location on the reference brain surface according to the surface correspondence established by the spatial normalization.

A mediation model was tested to assess the associations among hypoperfusion, cortical thinning, and AD diagnosis following the multiple regression approach described by [24]. First, AD diagnosis (i.e., the dependent variable, Y) was regressed on CBF_{PVE} (i.e., the independent variable, X): $Y \sim \beta_0 + \beta_1 X + \epsilon_1$. Then, the cortical thickness (i.e., the mediator, M) was regressed on CBF_{PVE}: $M \sim \alpha_0 + \alpha_1 X + \epsilon_2$. Finally, AD diagnosis was regressed on both the cortical thickness and CBF_{PVE}: $Y \sim \gamma_0 + \gamma_1 X + \gamma_2 M + \epsilon_3$. To establish that cortical thinning mediates cerebral hypoperfusion in its relationship with AD diagnosis, hypoperfusion should be associated with cortical thinning (i.e., significant non-zero α_1 regression coefficient) and there should be a significant reduction in the effect of CBF_{PVE} on the AD diagnosis in the final regression model. We used Sobel's significance test [24] based on a z-score defined as

$$z = \frac{\alpha_1 \gamma_2}{\sqrt{(\gamma_2^2 s_{\alpha_1}^2 + \alpha_1^2 s_{\gamma_2}^2)}}, \qquad (3)$$

where s_{α_1} and s_{γ_2} are the standard errors on α_1 and γ_2 estimates. Z-score reflects the effect size. Statistical computations were carried out using the statistical package R

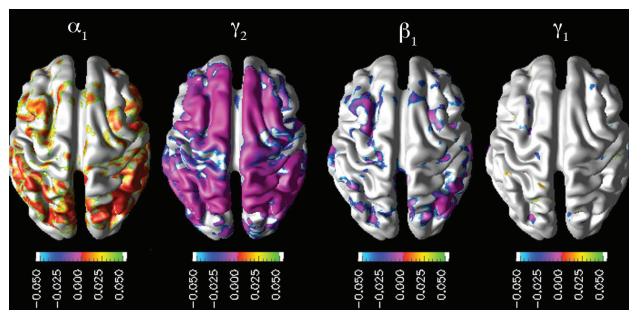Fig. 1. *Mediation model:* mappings of significant interactions.

(http://www.r-project.org/) and corrected for multiple comparisons, using false discovery rate (FDR) [25] at p<0.05.

III. RESULTS

Subject groups included healthy elderly (n=10), aged 50-71 years, and Alzheimer's disease patients (n=10), aged 51-69 years. Subjects were recruited from the Memory and Aging Center of the University of California, San Francisco. All subjects were diagnosed based upon information obtained from an extensive clinical history and physical examination. The MR images were used to rule out other major neuropathologies such as tumors, strokes, or inflammation but not to diagnose dementia. AD patients were diagnosed according to the criteria of the National Institute of Neurological and Communicative Disorders and Stroke-Alzheimers Disease and Related Disorders Association (NINCDS/ADRDA). All subjects or their guardians gave written informed consent before participating in the study, which was approved by the Committees of Human Research at the University of California at San Francisco.

For each subject, the structural MR image and perfusion MR images were processed following the framework described in the previous section. We then performed hypothesis testing to assess mediation effect of cortical thinning on the association between cerebral hypoperfusion and AD diagnosis. The key results from the multiple regression analyses listed in the methods section are shown in Fig. 1. α_1 map established the significant positive association between the cerebral hypoperfusion and cortical thinning in the parieto-temporal and frontal cortices. β_1 and γ_1 significance maps together illustrated the reduction in the effect of cerebral hypoperfusion on the AD diagnosis once the cortical thinning was entered to the model.

Sobel's significance test results in terms of z-scores is shown in Fig. 2. The mediator effect of cortical thinning on the association between cerebral hypoperfusion and AD diagnosis is observed bilaterally in the inferior parieto-temporal, superior frontal, and praecuneus cortices.

IV. CONCLUSIONS AND FUTURE WORKS

The ultimate goal of multi-modality MR image processing and analysis is to determine to what extent information from the various imaging modalities is redundant or complementary and how changes in various regions of the brain, detected by various modalities, interact with each other to produce cognitive and functional changes. Here, we presented a multimodality image processing framework to integrate unique
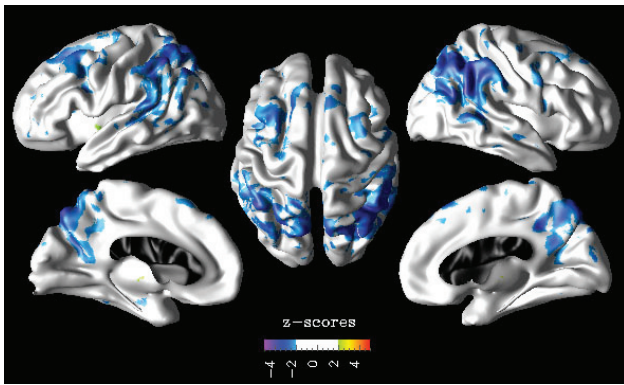
Fig. 2. *Sobel's significance test:* z-score reflecting the effect size of the mediation model.

and complementary observations on anatomical and physiological brain changes measured by different MR imaging modalities. A unique aspect to this study is that we performed a test on mediation hypothesis that requires a model based on measurements from two different MR imaging modalities (i.e., structural and perfusion MRIs). Our findings from these integrated multi-modality analysis were congruent with previously published results on neuropathology of AD patients.

Future studies should incorporate other MR modalities, such as diffusion weighted MRI (DWI), magnetic resonance spectroscopic imaging (MRSI). We advocate that each imaging modality provides unique and yet complementary information, contributing to better hypotheses and models regarding the neural systems involved in cognitive function, leading to improved diagnostic certainty.

V. ACKNOWLEDGMENTS

REFERENCES

[1] S. M. Smith, M. Jenkinson, H. Johansen-Berg, D. Rueckert, T. E. Nichols, C. E. Mackay, K. E. Watkins, O. Ciccarelli, M. Z. Cader, P. M. Matthews, and T. E. Behrens, "Tract-based spatial statistics: voxelwise analysis of multi-subject diffusion data," *Neuroimage*, vol. 31, pp. 1487–1505, 2006.

[2] G. B. Karas, E. J. Burton, S. A. Rombouts, R. A. van Schijndel, J. T. O'Brien, P. Scheltens, I. G. McKeith, D. Williams, C. Ballard, and F. Barkhof, "A comprehensive study of gray matter loss in patients with alzheimer's disease using optimized voxel-based morphometry." *NeuroImage*, vol. 18, pp. 895–907, 2003.

[3] H. Matsuda, N. Kitayama, T. Ohnishi, T. Asada, S. Nakano, S. Sakamoto, E. Imabayashi, and A. Katoh, "Longitudinal evaluation of both morphologic and functional changes in the same individuals with alzheimer's disease." *J. Nucl. Med.*, vol. 43, pp. 304–311, 2002.

[4] S. Minoshima, B. Giordani, S. Berent, K. A. Frey, N. L. Foster, and D. E. Kuhl, "Metabolic reduction in the posterior cingulate cortex in very early alzheimer's disease." *Ann. Neurol.*, vol. 42, pp. 85–94, 1997.

[5] N. A. Johnson, G. H. Jahng, M. W. Weiner, B. L. Miller, H. C. Chui, W. J. Jagust, M. L. Gorno-Tempini, and N. Schuff, "Pattern of cerebral hypoperfusion in alzheimer disease and mild cognitive impairment measured with arterial spin-labeling mr imaging: initial experience." *Radiology*, vol. 234, pp. 851–859, 2005.

[6] A. T. Du, G. H. Jahng, S. Hayasaka, J. H. Kramer, H. J. Rosen, M. L. Gorno-Tempini, K. P. Rankin, B. L. Miller, M. W. Weiner, and N. Schuff, "Hypoperfusion in frontotemporal dementia and alzheimer disease by arterial spin labeling mri," *Neurology*, vol. 67, pp. 1215–1220, 2006.

[7] A. Fellgiebel, M. J. Muller, P. Wille, P. R. Dellani, A. Scheurich, L. G. Schmidt, and P. Stoeter, "Color-coded diffusion-tensor-imaging of posterior cingulate fiber tracts in mild cognitive impairment," *Neurobiol Aging*, vol. 26, pp. 1193–1198, 2005.

[8] S. Takahashi, H. Yonezawa, J. Takahashi, M. Kudo, T. Inoue, and H. Tohgi, "Selective reduction of diffusion anisotropy in white matter of alzheimer disease brains measured by 3.0 tesla magnetic resonance imaging," *Neurosci Lett*, vol. 332, pp. 45–48, 2002.

[9] Y. Zhang, N. Schuff, G. H. Jahng, W. Bayne, S. Mori, L. Schad, S. Mueller, A. T. Du, J. H. Kramer, K. Yaffe, H. Chui, W. J. Jagust, B. L. Miller, and M. W. Weiner, "Diffusion tensor imaging of cingulum fibers in mild cognitive impairment and alzheimer disease," *Neurology*, vol. 68, pp. 13–19, 2007.

[10] S. Hayasaka, A. T. Du, A. Duarte, J. Kornak, G. H. Jahng, M. W. Weiner, and N. Schuff, "A non-parametric approach for co-analysis of multi-modal brain imaging data: application to alzheimer's disease," *NeuroImage*, vol. 30, pp. 768–779, 2006.

[11] G. I. D. Jong, R. A. D. Vos, E. N. Steur, and P. G. Luiten, "Cerebrovascular hypoperfusion: a risk factor for alzheimer's disease? animal model and postmortem human studies." *Ann N Y Acad Sci.*, vol. 826, pp. 56–74, 1997.

[12] J. C. de la Torre, "Critically attained threshold of cerebral hypoperfusion: can it cause alzheimer's disease?" *Ann N Y Acad Sci.*, vol. 903, pp. 424–436, 2000.

[13] — —, "Cerebral hypoperfusion, capillary degeneration, and development of alzheimer disease," *Alzheimer Dis Assoc Disord*, vol. 14, pp. S72–S81, 2000.

[14] G. H. Jahng, X. P. Zhu, G. B. Matson, M. W. Weiner, and N. Schuff, "Improved perfusion-weighted mri by a novel double inversion with proximal labeling of both tagged and control acquisitions." *Magn. Reson. Med.*, vol. 49, pp. 307–314, 2003.

[15] D. W. Shattuck and R. M. Leahy, "BrainSuite: An automated cortical surface identification tool," *Medical Image Analysis*, vol. 6, pp. 129–142, 2002.

[16] J. G. Sled, A. P. Zijdenbos, and A. C. Evans, "A non-parametric method for automatic correction of intensity non-uniformity in mri data," *IEEE Trans. Medical Imaging*, vol. 17, pp. 87–97, Feb. 1998.

[17] X. Han, D. L.Pham, D. Tosun, M. E. Rettmann, C. Xu, and J. L. Prince, "CRUISE: Cortical reconstruction using implicit surface evolution," *NeuroImage*, vol. 23, no. 3, pp. 997–1012, 2004.

[18] D. Tosun, M. E. Rettmann, S. M. Resnick, D. L. Pham, and J. L. Prince, "Cortical reconstruction using implicit surface evolution: Accuracy and precision analysis," *NeuroImage*, vol. 29, no. 3, pp. 838–852, 2006.

[19] A. J. Yezzi Jr. and J. L. Prince, "An Eulerian PDE approach for computing tissue thickness," *TMI*, vol. 22, no. 10, pp. 1332–1339, 2003.

[20] D. Tosun, S. Duchesne, Y. Rolland, A. W. Toga, M. Verin, and C. Barillot, "Analysis of cortical morphometry in differential diagnosis of parkinsons plus syndromes: Mapping frontal lobe cortical atrophy in progressive supranuclear palsy patients," in *10th International Conference on Medical Image Computing and Computer Assisted Intervention, Brisbane, Australia*, Nov 2007, pp. 281–289.

[21] C. J. Holmes, R. Hoge, L. Collins, R. Woods, A. W. Toga, and A. C. Evans, "Enhancement of mr images using registration for signal averaging," *J Comput Assist Tomogr.*, vol. 22, pp. 324–333, 1998.

[22] D. Tosun and J. L. Prince, "A geometry-driven optical flow warping for spatial normalization of cortical surfaces," *IEEE Trans. Medical Imaging*, 2008.

[23] P. Lorenzen, B. Davis, and S. Joshi, in *Proceedings of the Med Image Comput Comput Assist Interv Int Conf Med Image Comput Comput Assist Interv*, vol. 8, 2005, pp. 411–418.

[24] R. M. Baron and D. A. Kenny, "The moderator-mediator variable distinction in social psychological research: conceptual, strategic, and statistical considerations." *J. Pers. Soc. Psychol.*, vol. 51, pp. 1173–1182, 1986.

[25] Y. Benjamini and Y. Hockberg, "Controlling the false discovery rate: a practical and powerful approach to mltiple testing," *J. Royal Statistical Society*, vol. 57, pp. 289–300, 1995.